Chapter

A REGION-BASED ALGORITHM FOR AUTOMATIC BONE SEGMENTATION IN VOLUMETRIC CT

Authors[*]

Pedro L. Rodrigues[1], António H. J. Moreira[1], Jaime C. Fonseca[2], A.C. Pinho[3], Nuno F. Rodrigues[4,5], João L. Vilaça[1,4]

[1] Life and Health Sciences Research Institute (ICVS), School of Health Sciences, University of Minho, 4710-057 Braga, Portugal and ICVS/3B's - PT Government Associate Laboratory, Braga/Guimarães, Portugal

[2] Industrial Electronics Department, University of Minho, 4800-058 Guimarães, Portugal

[3] Mechanical Department, University of Minho, 4800-058 Guimarães, Portugal

[4] DIGARC – Polytechnic Institute of Cávado and Ave, Barcelos, Portugal

[5] DI-CCTC - University of Minho, 4710-057 Braga, Portugal

[*] E-mail address: pedrorodrigues@ecsaude.uminho.pt

Abstract

In Computed Tomography (CT), bone segmentation is considered an important step to extract bone parameters, which are frequently useful for computer-aided diagnosis, surgery and treatment of many diseases such as osteoporosis. Consequently, the development of accurate and reliable segmentation techniques is essential, since it often provides a great impact on quantitative image analysis and diagnosis outcome.

This chapter presents an automated multistep approach for bone segmentation in volumetric CT datasets. It starts with a three-dimensional (3D) watershed operation on an image gradient magnitude. The outcome of the watershed algorithm is an over-partioning image of many 3D regions that can be merged, yielding a meaningful image partitioning. In order to reduce the number of regions, a merging procedure was performed that merges neighbouring regions presenting a mean intensity distribution difference of ±15%. Finally, once all bones have been distinguished in high contrast, the final 3D bone segmentation was achieved by selecting all regions with bone fragments, using the information retrieved by a threshold mask. The bones contours were accurately defined according to the watershed regions outlines instead of considering the thresholding segmentation result.

This new method was tested to segment the rib cage on 185 CT images, acquired at the São João Hospital of Porto (Portugal) and evaluated using the dice similarity coefficient as a statistical validation metric, leading to a coefficient mean score of 0.89. This could represent a step forward towards accurate and automatic quantitative analysis in clinical environments and decreasing time-consumption, user dependence and subjectivity.

Introduction

Segmentation of bone tissue from images acquired with medical imaging modalities is an important component in many applications, such as bone densitometry, neurosurgical practice or bone-subtraction for assisted surgery. The rapid development and distribution of three-dimensional (3D) medical imaging technologies must be accompanied by advanced 3D analysis methods. Image acquisitions modalities used in radiology such as magnetic resonance imaging (MRI) or computed tomography (CT) are increasingly capable of generating high-resolution volumetric data sets. Commonly, these technologies produces images with a very wide dynamic range, where linear intensity window setting techniques must be used to provide adequate contrast and detail within specific imaged tissues such as bones, soft-tissues and lung detail.

The extraction of bone structures from the surrounding soft tissue is one of the most critical procedures to achieve 3D skeleton visualization. Such procedures have been simplified with the increase of CT high-resolution volumetric generation, and the definition of planar regions of interest to reduce the amount of processing data.

The bone segmentation can be manual or automatic. Manual segmentation is time-consuming, user-dependent, error-prone, subjective, and requires expert knowledge to yield accurate and robust results. In contrast, semi-automatic/automatic methods have the potential to provide fast, robust, user-independent and accurate segmentation. Semi-automatic/automatic approaches are required in today's challenging clinical environment.

The main difficulties in bone segmentation include ambiguity between the bone outline and the surrounding tissue or anatomic organ, irregular shape and size, different anatomic locations and patient conditions, presence of neighboring structures/organs

with the same density/values, non-uniformity of bone tissue (ranging from dense cortical bone to textured spongy bone), small inter-bone spaces and the inherent blurring of CT imaging. Due to these multiple difficulties, new methods represent a nontrivial task and sometimes seem to be inadequate.

According to the literature [1] fully automated methods rely upon manual post processing, since the performance of image processing algorithms is often sensitive to noise and image contrast. Some pre-processing is usually necessary to achieve more efficiency in detecting weak edges and suppress others caused by noise. A variety of editing tools were developed [1] to correct or improve results of initial automatic segmentation procedures: hole-filling, point-bridging, and surface-dragging.

Semi-automatic approaches have also been proposed for different actors. The most conventional techniques are based on thresholding algorithms by manually or automatically selecting a Hounsfield Unit (HU). The major drawbacks of these algorithms reside on the global thresholding procedure, which does not consider local gray value variations within bone structure, and adaptive thresholding occasionally results in the merging of small gaps between bones [2-5]. The performance of this methods are highly dependent on image quality acquired from the medical imaging modalities and material density, single thresholds tend to fail in providing correct segmentations in more complex scenarios. Consequently, too large segmentation occurs if the threshold is too low to define the boundary line, too far away from the real bone boundary. On the other hand, a bone structure becomes too small for higher thresholds, because the boundary line cuts away some of the bone.

Therefore, intensity based algorithms have advantages, such as the speed in the case of global thresholding, and disadvantages, like the need for post-processing like edge linking, depending on the CT volumetric data sets quality.

Consequently, better segmentation results are achieved by combining thresholding methods with other image processing algorithms [6]. A highly automated 3D based method for bone segmentation in volumetric CT datasets, was developed in [7]. They use a multistep approach starting with region-growing and local adaptive thresholds, followed by procedures to correct bone boundary discontinuities. Zhou et al. [8] developed a computer-aided diagnosis scheme for automatically segment skin, soft tissue and bone structures from high-resolution torso CT images. This method was based on gray-level threshold to separate the regions of interest from the background. The skeleton was segmented by a region growing process using an optimal threshold value. A ray casting algorithm presented in [9] overcome threshold drawbacks, by using a gray value gradient, which is also not affected by gray value variations with low frequencies.

Other segmentation methods described in the literature use the combination of region-based, edge-based and deformable algorithms to improve segmentation procedures. In [2], the authors use a method based on region growing from initialized seeds, where growth is modulated by a skeletally-mediated competition between neighbouring regions. This method combines the advantages of deformable models with region growing and region competition. Hahn presents an interactive watershed transform to separate bone from white matter in an MRI. The use of watersheds to segment objects of interest in images often produce more stable results as well as continuous segmentation boundaries, independently of image contrast or noise level [10, 11].

Most of these methods have some limitations, as they are relatively slow, not very accurate and highly computationally-intensive particularly for large images. Moreover, the segmentation of image regions is still one of the major bottlenecks, especially for 3D image analysis, as most segmentation approaches are 2D based. The segmentation of 3D structures from 2D results are error prone, most often require intensive user interactions and neglect the three-dimensional character of the structures to be segmented.

In this work, a fully 3D automated method is proposed, based on a watershed operation that is applied to the image gradient magnitude. The result of the watershed operation, an image with several primitive regions, was input to a merging procedure that selectively merges similar regions and maintains the relevant bone boundaries. The final bone segmentation was achieved by automatic select the merged regions with the information retrieved by a threshold mask. The implemented strategy is independent of image specific parameters and can also be applied in images from different imaging modalities allowing it to be used by clinical experts.

This chapter is organized as follows: the next sub-chapter describes all algorithms used to segment the bone structures; then it is presented and discussed some simulation and statistical results followed by the main conclusions.

Methods

Since the segmentation of images into meaningful regions has been an important area in medical image analysis, the implemented strategy is based on (1) image partitioning into small primitive regions, (2) region merging and (3) the selection of merged regions using information provided by a threshold mask.

To verify the suitability of the proposed method, tests were run on CT images acquired at São João Hospital of Porto (Portugal), according to the ethical review board of the University of Minho. The tests were conducted on 185 CT data sets from different patients. Each CT slice size has 512 x 512 pixels, with a slice thickness of 5 mm. The pixel resolution ranged from 0.46 to 0.84 mm (for both vertical and horizontal directions). An overview of the different stages of the method is given in Fig. 1.

Pre-Processing

The aim of this stage was to calculate an image partitioning within several primitive 3D regions.

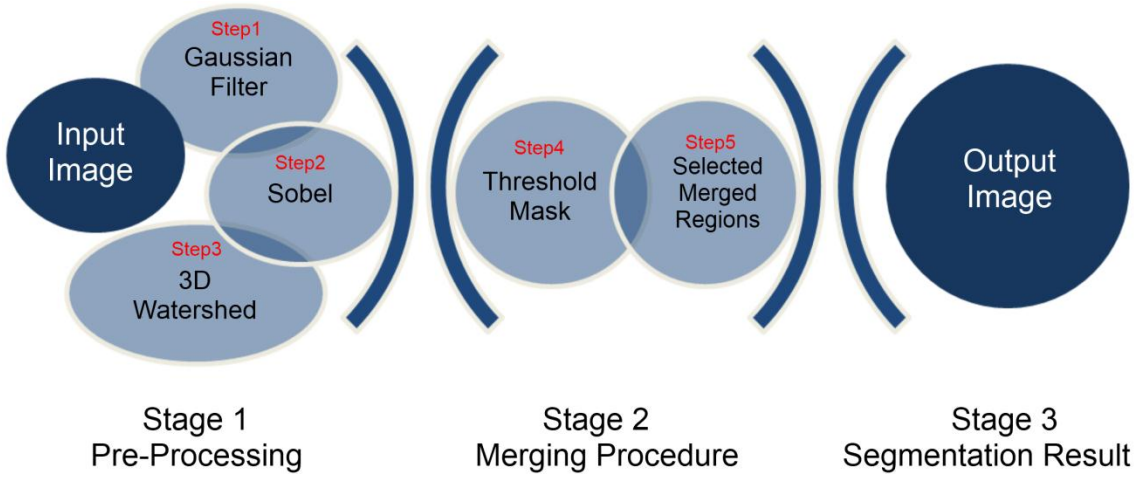

Fig. 1. Block diagram giving an overview of the different bone segmentation steps.

Due to the stochastic processes during the image creation, noise is always present. Therefore the meaningful information of an image object can be lost if the noise level is too high compared with the object intensity. To this extent, the noise corrupting the image was initially reduced using a Gaussian filter (Fig. 1, Stage 1, Step 1).

The Gaussian filter was implemented as in [21] to reduce the image noise. Considering $f(x, y)$ a two-dimensional function, the Gaussian filter is a 2D low-pass transformation which performance depends on the standard deviation of the filter. In this work, the standard deviation was experimentally calculated with a final value of 1.8 pixels, allowing an output image with a right equilibrium between smoothing and edge details.

Then, the gradient of the smoothed image is calculated using the Sobel operator. This operator is used in image processing, particularly within edge detection algorithms. Technically, it works as a similarity measure, computing an approximation of the gradient ∇f of the image intensity function f. Mathematically, the gradient ∇f is at each image voxel a 3D vector with the components given by the derivatives in all directions (Fig. 1, Stage 1, Step 2) [12, 13].

The magnitude outcome of the Sobel operator was input to a 3D watershed algorithm to segment the bone regions (Fig. 1, Stage 1, Step 3). Briefly, the watershed operation assigns different labels to whole pixels that are separated by an image edge. Although many techniques have been suggested for edge detection, which performances are very sensitive to noise and image contrast. The use of watersheds often produce more stable segmentation results as well as continuous segmentation boundaries, independently of image contrast or noise level [14-16].

The probability that a single region will suitably associate to each object of interest is small. Knowing this limitation, a good design goal was to create several small primitive regions and try to semantically link them into a hierarchy. An optimal number of regions are essential to achieve a good segmentation.

Thus, pixels that are separated by an image edge, which correspond to a gradient magnitude ridge, will be assigned a different label. In order to create the segmentation primitives correctly, the following restrictions are all considered:

1. After creating the primitive regions, every pixel must be in a region;
2. $R_i \cap R_j = \emptyset$ for all i and j, $i \neq j$, indicating that the regions must be disjoint;

3. $P(R_i) = \text{TRUE}$ for $i = 1,2,\ldots,n$, which means that properties in a segmented region must be satisfied by the pixels;
4. $P(R_i \cup R_j) = \text{FALSE}$ for $i \neq j$, indicates that regions R_i and R_j are different in the sense of predicate $P(R_i)$;
5. A pixel p, which is a boundary pixel, belongs to the region $R_{(p)}$ if there is at least one pixel q in the 4-connected in 2D (or 6-connected in 3D) neighbourhood of p that does not belong to $R_{(p)}$. This pixel *q* is a boundary pixel of its region $R_{(q)}$ and the common pixel boundary of p and q is a boundary line element (in 2D, or surface element in 3D) of $R_{(p)}$ and $R_{(q)}$;
6. The boundary between two regions is the union of all their common boundary elements.

Considering these restrictions, in this work watershed regions were labeled by a starting point and following the flow line, whose direction was the gradient of intensity to a local minimum: for each pixel *p* in the image, it was created a gradient path between *p* and *q*, where *q* is the pixel on the 27-neighborhood of *p* with the smallest gradient magnitude. Each time that there is no pixel *q* in *p*' neighbourhood with smaller gradient magnitude, the pixel *q* is marked as a local minimum of the gradient magnitude and assigned a distinct label. The process continues until all image volume is processed (Fig. 2).

In the end, the whole image is segmented into primitive regions and the quality of the watershed segmentation results will depend on:

1. The number of pixels of the same object that are within one region;
2. The ratio of image edges that correspond to regions edges.

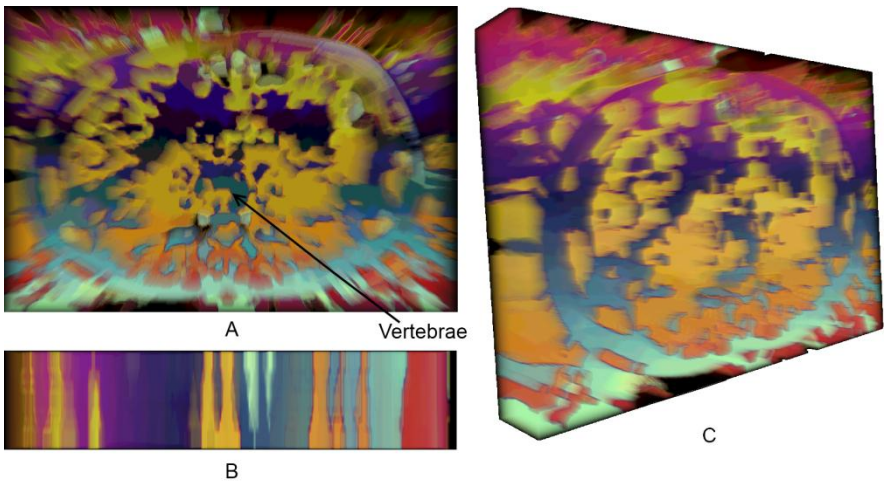

Fig. 2. 3D watershed operation result: the colour map illustrates the region extension along X, Y and Z directions.

Merging Procedure

As shown in (Fig. 2), the output of the watershed algorithm is an oversegmented image, containing a set of non-overlapping regions. Although oversegmentation increases the

probability for a region boundary to correspond to boundaries of important objects, it can also create many insignificant boundaries.

This section describes how the 3D bone structures were automatically determined. Briefly, this procedure consisted on the identification of regions edges and its connections with similar intensity, ignoring all other regions with wide mean intensity variations. It assumes that:

- All pixels within the same region are homogeneous;
- Regions within bone regions have homogeneous intensity variations;
- Regions within bone regions are considerably different from other outside neighbouring regions;
- R_i with $i=1,2,3,\ldots,n$ is a connected region, which means that a region must be connected to their neighbourhood region in some predefined sense;

Since all pixels within the same region are homogeneous and considerably different from other neighbouring regions, there are neighbouring regions belonging to the bone structures that could be merged, yielding to a meaningful image partitioning.

After establishing the image segmentation through the application of the watershed algorithm, this merging procedure performs feature identification in each region, by identifying the centroid, mean intensity distribution, minimum and maximum values, region edges, and edges region neighbours.

Each time two neighbourhood regions present a mean intensity distribution difference of ±15%, these two regions are merged and the edge between them is removed. Different merged results from the input image (Fig. 3 A) can be obtained when different percentage similarities are used - Fig. 3 B.

The bone segmentation was finally achieved by selecting all regions with bone fragments, using the information retrieved by a threshold mask (Fig. 3 - C and Fig. 1 - step3). This level was calculated through a basic threshold algorithm, using a value higher than the one that was needed to precisely identify the bone outlines (0.9/1 threshold level). All regions that possessed white pixels on their interior, corresponding to bone regions, were chosen as final result (Fig. 3 D).

The bone outline was defined by only taking into account the information of the region contours after the merging process; thus, the segmentation result was not influenced by the threshold value that determines the bone outline thickness.

3D reconstructions of two patients are shown in Fig. 4. The colour map illustrates the differences between the regions produced by the watershed algorithm and the binary image used for the regions selection after fusion.

These differences were computed using a Ray-Triangle intersection method, which was used to compute the minimal distance between two triangle meshes: the bone structure constructed using the threshold mask (Ts) and the bone structure acquired using the proposed method (Tp).

For each triangle facet of the Tp(i) (with i = 0, 1, 2,… N, with N being the total number of triangles on the bone structure), a ray R(i) was defined with the Y direction (Fig. 4 (c)), starting at a point Pi(i) within Tp(i) and ending at a Pf(i) (point above bone structure from the threshold mask). Then, its intersection with Ts(j) (with j = 0, 1,2,… Nt, with Nt being the total number of mesh triangles) was checked.

Based on these distances, the bone structure facets from the watershed algorithm were colored according to the color-map defined on the color bar in Fig. 4.

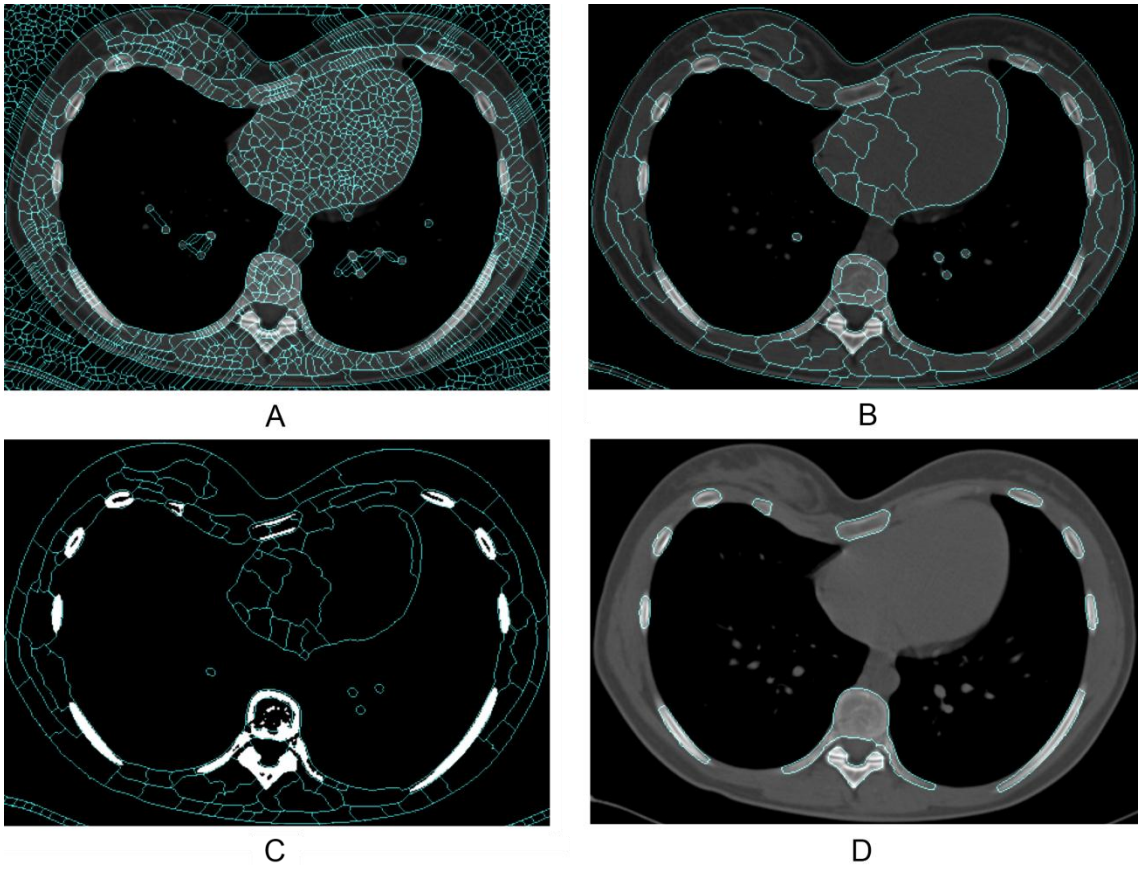

Fig. 3. Representation of the bone segmentation procedure outline: A) watershed operation result in a 2D image; B) merging procedure (15% of difference between regions); C) Threshold masks to automatically select all the regions belonging to the bone regions; D) final segmentation result.

Fig. 4. 3D reconstructions of the anterior chest bones of two patients.

Results

A proper estimation of bone volume and structure are useful for several applications such as computer-aided diagnosis, surgery and treatment response evaluation. Due to the limited number of images available for each patient, clinical planning and quantitative monitoring of disease evolution requires fast segmentation methods with high reproducibility. Thus, this chapter introduces a segmentation methodology to automatic segment bone regions.

The segmentation procedure was reduced by selecting merged regions of a watershed operation using the information retrieved by a threshold mask. Therefore, the total number of decisions to segment bone structures was drastically reduced, increasing segmentation efficiency and robustness and decreasing time-consumption, user dependence, and subjectivity. The observer variability also decreased since all regions were computed automatically without any user intervention.

The merging procedure was used to selectively merge watershed regions based on their image mean intensity distribution. However, a proper segmentation can only be accomplished with an optimal number of regions since such a sequence of merges does not guarantee the construction of an optimal image partitioning. False merges depends both on size of the regions to be merged and on the noise present in the image.

A small number of regions with larger granularity (higher merging percentage difference) can be used for fast and rough segmentations of big bones; while a higher number of regions with smaller granularity (small merging percentage difference) should be used to segment smaller bones. Although the segmentation procedure is automatic, the user can always erase and produce detailed segmentation by manually selecting regions of interest. Fig. 5 shows results of different merging procedures according to different merging percentage differences.

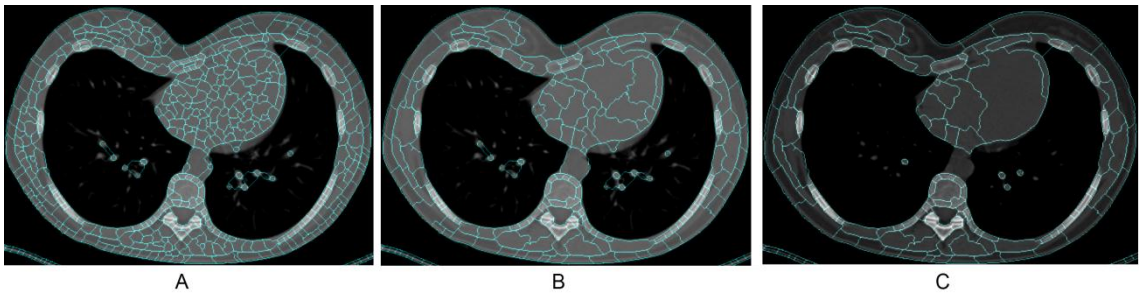

Fig. 5. Merging procedure results with different merging percentage differences: A -5%, B – 10% and C – 5%.

The number of watershed regions was also dependent on the standard deviation of the Gaussian filter value. High standard deviation values may destroy some image details and object boundaries, which cannot be recovered at the merging stage. This is justified from the fact that when the standard deviation value is high, the noise reduction algorithm may over-smooth part of the image intensity discontinuities, resulting in low magnitudes.

Therefore, the segmentation procedure could be interpreted as an optimization problem of some parameters (standard deviation Gaussian filter value, percentage value to merge watershed regions and the threshold values mask) in order to reduce unsatisfactory results as “undermerged” or “overmerged” segmented results.

The quality and performance of the segmentation quality of this work was evaluated using the Dice Similarity Coefficient (DSC) metric. It measures the spatial overlap between two segmentation results: automated segmentation result (A) and manual segmentation (B). As indicated by Zijdenbos [17] a good overlap occurs when DCS > 0.7. For each segmentation (A, B) the DSC was determined showing a mean value of 89% (range from 73% to 96%) with a standard deviation equal to 4.9%. A total of 185 CT data sets were used in this study, comprising patients with different pathologies and different image intensities.
Although DSC is quite simple to interpret, there are several limitations in using DCS as an overlap measures since it is not robust in terms of size of the target. For small tumors others metrics might be considered like ROC analysis, odds ratio or distance measures.

Conclusion

An automatic algorithm was presented for bone segmentation in CT images. The segmentation was reduced by selecting all merged regions belonging to the bone structure using the information retrieved by a threshold mask. This procedure showed high sensitivity detecting bone boundaries located near other anatomical structures, identifying weak edges, robustness against image noise, and being able to segment hyperdense and hypodense bones with different size and shape.
Best results were achieved when an optimal number of regions were created depending on the percentage value to merge watershed regions and the standard deviation Gaussian filter value.
The proposed segmentation technique was implemented for 2D and 3D cases, producing successful results in the 2D performance and execution. Further work is needed in the 3D merging procedure and also in the evaluation of the method by clinical experts. Hereupon, new research paths based on this work have to be investigated. For example, this algorithm should be tested and validated in other bone structures besides the rib cage in order to increase and validate the algorithm suitability.

Acknowledgment

The authors acknowledge to Foundation for Science and Technology (FCT) - Portugal for the fellowships with the references: SFRH/BD/74276/2010; SFRH/BD/68270/2010; and, SFRH/BPD/46851/2008. This work was also supported by FCT R&D project PTDC/SAU-BEB/103368/2008.

References

[1] Y. Kang, *et al.*, "Interactive 3D editing tools for image segmentation," *Medical Image Analysis*, vol. 8, pp. 35-46, 2004.
[2] T. B. Sebastian, *et al.*, "Segmentation of carpal bones from CT images using skeletally coupled deformable models," *Medical Image Analysis*, vol. 7, pp. 21-45, 2003.

[3] M. N. Coleman and M. W. Colbert, "Technical note: CT thresholding protocols for taking measurements on three-dimensional models," *Am J Phys Anthropol,* vol. 133, pp. 723-5, May 2007.

[4] R. J. Fajardo, *et al.*, "Nonhuman anthropoid primate femoral neck trabecular architecture and its relationship to locomotor mode," *Anatomical Record-Advances in Integrative Anatomy and Evolutionary Biology,* vol. 290, pp. 422-436, Apr 2007.

[5] T. N. Hangartner, "Thresholding technique for accurate analysis of density and geometry in QCT, pQCT and microCT images," *J Musculoskelet Neuronal Interact,* vol. 7, pp. 9-16, Jan-Mar 2007.

[6] L. I. Wang, *et al.*, "Validation of bone segmentation and improved 3-D registration using contour coherency in CT data," *Ieee Transactions on Medical Imaging,* vol. 25, pp. 324-334, Mar 2006.

[7] Y. Kang, *et al.*, *A new accurate and precise 3-D segmentation method for skeletal structures in volumetric CT data* vol. 22. New York, NY, ETATS-UNIS: Institute of Electrical and Electronics Engineers, 2003.

[8] X. R. Zhou, *et al.*, "Automated segmentations of skin, soft-tissue, and skeleton from torso CT images," *Medical Imaging 2004: Image Processing, Pts 1-3,* vol. 5370, pp. 1634-1639
2158, 2004.

[9] H. Scherf and R. Tilgner, "A new high-resolution computed tomography (CT) segmentation method for trabecular bone architectural analysis," *American Journal of Physical Anthropology,* vol. 140, pp. 39-51, 2009.

[10] L. Vincent and P. Soille, "Watersheds in digital spaces: an efficient algorithm based on immersion simulations," *IEEE Transactions on Pattern Analysis and Machine Intelligence,* vol. 13, pp. 583-598, 1997.

[11] H. K. Hahn, "Morphological Volumetry: Theory, Concepts, and Application to Quantitative Medical Imaging," PhD thesis, University of Bremen, 2005.

[12] R. O. Duda and P. E. Hart, Eds., *Pattern Classification and Scene Analysis*. New York, 1973, p.^pp. Pages.

[13] I. N. Bankman, "Segmentation," in *Handbook of Medical Image Processing and Analysis (Second Edition)*, N. B. Isaac and PhD, Eds., ed Burlington: Academic Press, 2009, pp. 71-257.

[14] Z. Peter, *et al.*, "A constrained region growing approach based on watershed for the segmentation of low contrast structures in bone micro-CT images," *Pattern Recognition,* vol. 41, pp. 2358-2368, 2008.

[15] C. R. Jung and J. Scharcanski, "Robust watershed segmentation using wavelets," *Image and Vision Computing,* vol. 23, pp. 661-669, 2005.

[16] F. C. Flores and R. d. A. Lotufo, "Watershed from propagated markers: An interactive method to morphological object segmentation in image sequences," *Image and Vision Computing,* vol. 28, pp. 1491-1514, 2010.

[17] A. P. Zijdenbos, *et al.*, "Morphometric analysis of white matter lesions in MR images: method and validation," *Medical Imaging, IEEE Transactions on,* vol. 13, pp. 716-724, 1994.